Cement and Concrete Research 39 (2009) 324–328

Contents lists available at ScienceDirect

Cement and Concrete Research

journal homepage: http://ees.elsevier.com/CEMCON/default.asp

Embedded NMR sensors to monitor evaporable water loss caused by hydration and drying in Portland cement mortar

P.F. de J. Cano-Barrita [a,b,c,*], A.E. Marble [a], B.J. Balcom [a,*], J.C. García [a], I.V. Masthikin [a], M.D.A. Thomas [b], T.W. Bremner [b]

[a] MRI Centre, Department of Physics, University of New Brunswick, Fredericton, NB, Canada E3B 5A3
[b] Department of Civil Engineering, University of New Brunswick, Fredericton, NB, Canada E3B 5A3
[c] CIIDIR IPN Unidad Oaxaca, Hornos 1003, Sta. Cruz Xoxocotlan, Oaxaca, Mexico

ARTICLE INFO

Article history:
Received 21 July 2008
Accepted 20 January 2009

Keywords:
A: Drying
Hydration
B: Pore size distribution
E: Mortar
Embedded NMR sensor

ABSTRACT

Providing adequate moisture content in cement-based materials is important during hydration of the cement paste to ensure proper development of their mechanical and durability properties. Subsequently, water is involved in the deterioration of concrete either as a pure liquid or by carrying aggressive species. This paper explores the use of small embedded NMR sensors to monitor evaporable water loss in Portland cement mortars. Results indicate that these sensors are effective in detecting loss of evaporable water due to hydration and drying. During drying, the mass loss is linearly proportional to the NMR signal loss. In addition, the amount of evaporable water detected with the sensor has a good correlation with the amount of evaporable water in a companion specimen tested in a traditional low field magnet by NMR and by gravimetric measurements.

1. Introduction

Moisture plays an important role in the entire life cycle of concrete structures. At early age, moisture is needed to hydrate the cement particles to develop appropriate mechanical and permeability properties to withstand the applied loads and environmental action. In almost all the degradation mechanisms of concrete, water is present. For instance, water is involved in drying shrinkage cracking, ingress of aggressive species, corrosion of reinforcement, and freezing and thawing, and internal chemical reactions such as alkali–silica reaction [1].

There are standard methods to measure the moisture condition in field concrete, such as relative humidity probes [2]. However, in field concrete it is difficult to obtain accurate measurements of relative humidity because of its temperature dependence. Although relative humidity can be used as an indicator when surface coverings or treatments can be applied to concrete floors [3]. Other common methods used as indicators of the water content in floors include the "Calcium Chloride Vapour Emission Test", which quantifies the moisture vapour emission rate (MVER) of a concrete subfloor [4]. It involves placing anhydrous calcium chloride crystals beneath a plastic dome for 60 to 72 h. The crystals absorb vapour in the air inside the dome and the difference between the initial and final weight of the crystals is used to determine the MVER in pounds of water/thousand square feet of surface/24 h.

In a porous media, NMR/MRI is the most effective non-destructive and non-invasive technique that has been used to undertake NMR relaxation time studies of hydrating cement based materials [5–7]. In addition, the moisture distribution during drying [8,9], capillary water absorption [10] as well as the effects of drying and freeze-thaw cycling can be studied [11]. Recently, mobile NMR equipment has been used for porosity analysis of rock cores [12] and cement-based materials [13]. Coils embedded in a sample and placed in the stray field of a superconducting magnet have been used to obtain one-dimensional profiles in mortar samples [13]. Unilateral magnet design has widened the applications for NMR in samples with a large size [14,15].

This paper presents preliminary results on the use of miniature NMR sensors to monitor moisture changes in Portland cement mortar caused by hydration and drying, as well as pore size refinement. Other potential applications include measuring the water content in fresh concrete, sand, and soils.

2. Experimental

2.1. Miniature NMR sensors

Construction of the miniature NMR sensors [15] is depicted in Fig. 1. The radio frequency (RF) coil is etched on a printed circuit board and tuned to the Larmor frequency with small, fixed value, capacitors. The RF coil sits atop a stack of two NdFeB disk magnets. Thin iron disks were used below the magnets to adjust the magnetic field strength to

* Corresponding authors.
E-mail addresses: pcano@ipn.mx (P.F. de J. Cano-Barrita), bjb@unb.ca (B.J. Balcom).

0008-8846/$ – see front matter © 2009 Elsevier Ltd. All rights reserved.
doi:10.1016/j.cemconres.2009.01.011

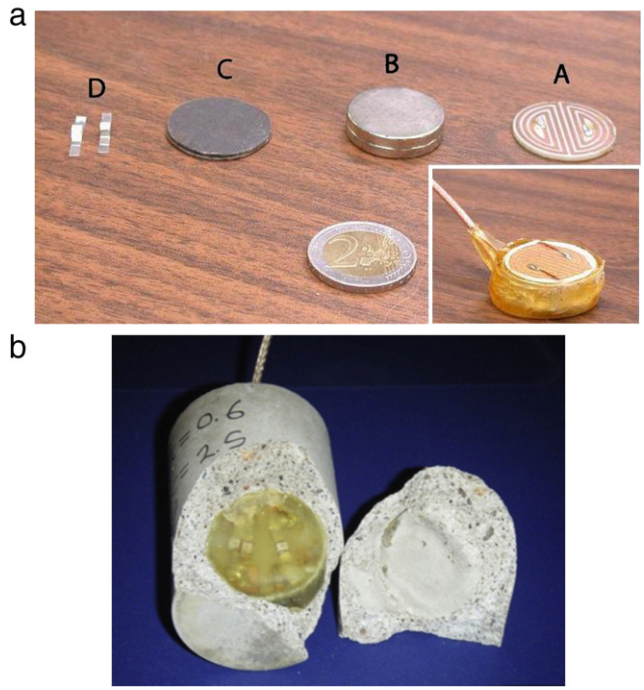

Fig. 1. a) Miniature NMR sensor construction (Marble *et al.*, 2007). A RF coil (A) etched on a printed circuit board sits atop a stack of disk magnets (B). Iron disks (C) below the magnets are used to adjust the field strength above (≈0.24 T). The RF coil is tuned to the Larmor frequency (≈10.2 MHz) with small capacitors (D) mounted to a PC board below the magnets, and fed through a thin coaxial cable. The 2 Euros coin is shown for scale, b) NMR sensor (30 mm in diameter and 12 mm in height) embedded in a Portland cement mortar specimen (diameter = 40 mm).

approximately 0.24 T, which produces a ^{1}H Larmor frequency of 10.2 MHz. The sensor is connected to a 2.5 mm diameter coaxial cable, and encased in waterproof epoxy resin. The final sensor dimensions are 30 mm in diameter and 12 mm in height.

Fig. 2 shows the measured magnetic field magnitude in a miniature NMR sensor. Two mm above the magnet the field is ≈0.25T. The inhomogeneous B_0 and B_1 fields define a local sensitive region in which bulk relaxation times or diffusion measurements can be undertaken.

Small variations in the magnetic field strength of the magnets used to fabricate the sensors change the resonant frequency and determine its NMR sensitivity. After fabrication, each sensor was tested to determine its sensitivity with respect to others, by placing a small piece of elastomer on it and obtaining the NMR signal, which was used to normalize the results obtained with different sensors. Alternatively, one could immerse the sensors in $CuSO_4$ doped water (T_1 and $T_2 \approx 3$ ms) to obtain the NMR signal.

The basic idea is to place these sensors in fresh concrete and monitor the changes in water content caused by hydration/drying over time. In future work we will attempt to correlate the T_2 values with the compressive strength of hardened concrete through the pore size characteristics.

2.2. Measuring technique

The Carr–Purcell–Meiboom–Gill (CPMG) NMR measurement, suitable to measure NMR signals in inhomogeneous magnetic fields, was used to obtain the $T_{2\text{eff}}$ decay envelope (Fig. 3). The $T_{2\text{eff}}$ relaxation data was fitted to Eq. ((1) and back extrapolated to determine the signal amplitude, M(0), which is proportional to the amount of water in fresh cement paste and in hardened mortar specimens.

$$M(t) = M(0) \cdot e^{-\frac{t}{T_{2eff}}} \quad (1)$$

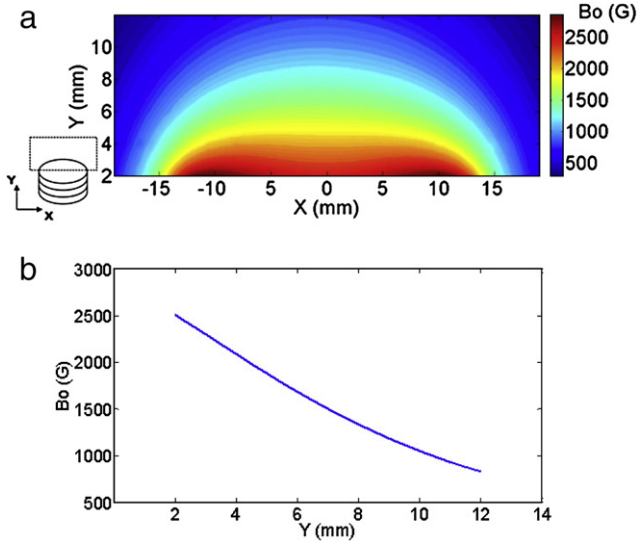

Fig. 2. a) Measured magnetic field magnitude (B_o) above the RF coil of the sensor. Notice the inhomogeneous nature of the magnetic field, b) Magnetic field variation along the *Y* direction at the center of the magnet ($X = 0$ mm). The calculated magnetic field gradient is 2000 G/cm in the region of space from 2–7.5 mm above the RF coil.

2.3. Cement paste mixes and mortar specimens

Type I Portland cement and distilled water were used to prepare cement pastes at different w/c ratios (0.35, 0.40, 0.45, 0.50, 0.55, and 0.60) to measure the NMR signal with the sensors using the CPMG measurement. This was done to determine the ability of the sensors to detect different water concentrations in fresh cement paste.

Cylindrical mortar specimens (w/c ratios of 0.60 and 0.45) measuring 40 mm in diameter and 50 mm in length were cast. The mortar was prepared using Type I Portland cement, river sand (specific gravity = 2.59 and absorption = 1.1%), and distilled water. The sensors were located approximately in the center of the specimen. A companion cylinder for each w/c ratio was cast for measurement on an ordinary permanent magnet NMR instrument to determine the T_2 decay curve.

After casting, the specimens were kept sealed at 23 °C to avoid significant loss of water due to drying, so that the evaporable water loss observed during the NMR measurements was mainly caused by hydration of cement. A few hours after casting, a Bruker Minispec spectrometer was used with the sensors to obtain the NMR signal. At the same time, the companion specimens were tested in another Bruker Minispec spectrometer at 6.25 MHz., in which the T_1, T_2, and T_2^* relaxation times in the mortar w/c = 0.60 were measured at 0, 3, 24, and 168 h.

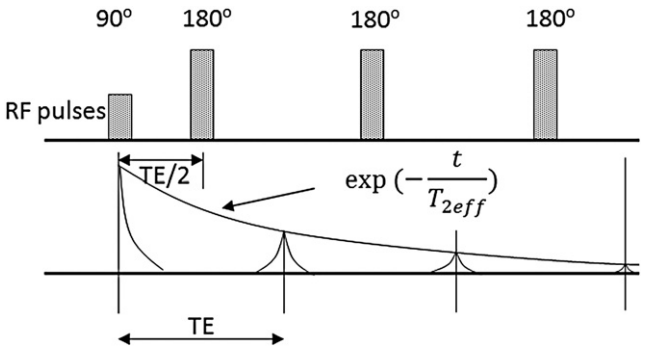

Fig. 3. CPMG measurement for NMR signal detection with the miniature sensors. TE is the echo time and $T_{2\text{eff}}$ is the effective transverse relaxation time. The initial echo amplitude is proportional to the amount of water in the sample. The pulse width of the 90° and 180° radio frequency (RF) pulses was the same, only the power was changed.

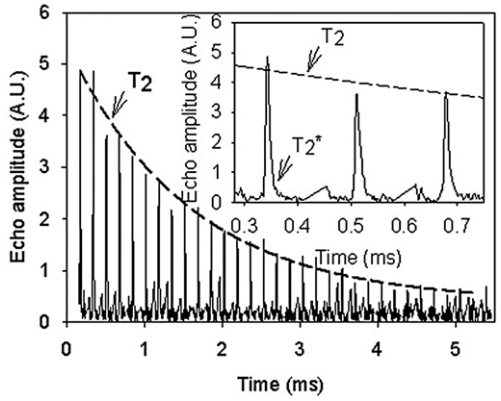

Fig. 4. CPMG echo train obtained with the miniature NMR sensor. The acquisition parameters were TE = 0.168 ms, TR = 0.20 s, 32 echoes, 8192 scans, $pw_{90°}$ (half power) and $pw_{180°}$ (full power) = 3.85 μs. Acquisition time = 30 min.

At the end of testing the specimens were dried at 60 °C, lower than the maximum operating temperature of the magnets (121 °C). Then the specimens were vacuum saturated with water and the CPMG experiment was repeated.

3. Results and discussion

Fig. 4 is a typical echo train obtained with the miniature NMR sensors in Portland cement mortar. An enlarged view of the echoes is shown on the right hand side of the graph. The data was acquired at a point sampling rate of 1 MHz, which is more than six times the frequency range of the band pass filter used (0.15 MHz). The Nyquist theorem requires a point sampling rate at least two times this maximum frequency. The scatter observed in the peak amplitudes is caused by the inhomogeneous B_0 and B_1 magnetic fields from the unilateral magnet and the butterfly type of RF probe used, respectively. Repeated measurements with a specific sensor on the same sample yielded less than 1% standard deviation. We do not have data obtained with a mobile NMR scanner on the same materials to compare the repeatability and it will be determined in future work.

Fig. 5 represents the relationship between the NMR signal and the amount of water in cement pastes at different w/c ratios. There is a linear relationship between these variables and the intercept is near the zero crossing, demonstrating the ability of the sensors to quantitatively detect different water concentrations in fresh cement paste samples.

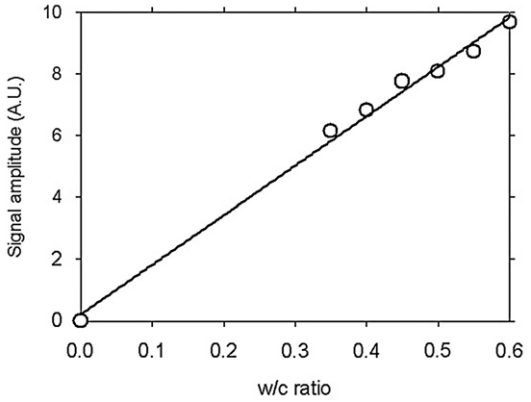

Fig. 5. Relationship between the signal amplitude back extrapolated to time zero in the CPMG decay and the amount of water in ordinary Portland cement pastes ($r^2 = 0.997$). Six discrete samples were measured. The CPMG acquisition parameters were TE = 0.168 ms, TR = 0.20 s, 32 echoes, 2048 scans. Acquisition time = 7.5 min/point.

Table 1
Relaxation times of mortar w/c = 0.60 measured with a Bruker Minispec permanent magnet at 0.15 T (6.25 MHz).

Time (h)	NMR Relaxation time constant		
	T_1 (ms)	T_2 (ms)	T_2^* (μs)
0	28	12	89
3	20.2(95%)	20.4(19%)	87
	1.4(5%)	7.5(81%)	
24	2.9(65%)	4.3(33%)	77
	0.5(35%)	1.1(67%)	
168	2.0(43%)	2.6(28%)	64
	0.4(57%)	0.4(72%)	

Relaxation time distributions were fit to a bi-exponential model. The percentage indicates the contribution of each component.

The T_1, T_2, and T_2^* relaxation times for the mortar w/c = 0.60, measured in the homogeneous magnetic field of an ordinary Bruker Minispec permanent magnet are shown in Table 1. For mortars with a lower w/c ratio, these relaxation times would be even shorter. The same trends will apply to the case of concrete made with common materials like ordinary Portland cement, river/crushed coarse and fine aggregates. Observe that T_2^*, which is related to the NMR signal lifetime, does not change significantly from the fresh to hardened state. However, the changes in T_1 and T_2, which can be related to microstructural characteristics such as surface/volume (S/V) ratio of the pores, are one order of magnitude smaller.

On the other hand, in inhomogeneous magnetic fields such as those present in the miniature sensor, the T_2^* relaxation time will be as

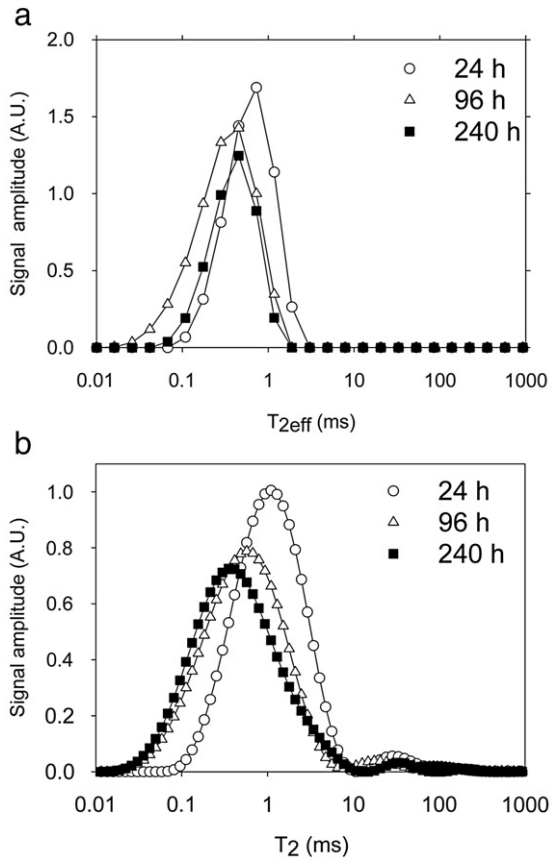

Fig. 6. Change in the T_{2eff} distribution over time in a sealed hydrating mortar specimen w/c = 0.60 at 23 °C, obtained by regularized inverse Laplace Transformation with the UPEN program, a) with embedded magnet and b) with an ordinary magnet NMR measurement. As the sample hydrates, the mean pore size distribution decreases as indicated by the reduction of T_{2eff}. A distribution is obtained because of the distribution of pore sizes in all cases.

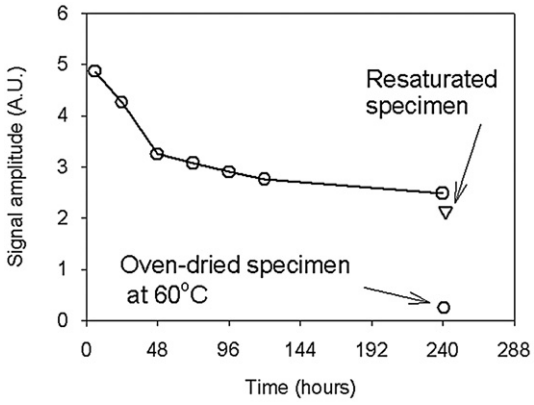

Fig. 7. Evaporable water signal loss during hydration of a sealed Portland cement mortar specimen (w/c = 0.60).

short as 6 μs, estimated from the T_2^* decay in the echoes (Fig. 4). This makes the measurement of T_1 and T_2^* impractical with the miniature sensors and the only possible manner to characterize the water content and microstructure of the porous material is through T_2 measurements.

In inhomogeneous magnetic fields the CPMG measurement gives the following effective T_2 decay constant [12],

$$\frac{1}{T_2} = \frac{1}{T_{2,b}} + \rho_2 \cdot \frac{S}{V} + \frac{D \cdot (\gamma GTE)^2}{12} \quad (2)$$

where ρ is the relaxivity of the pore surface, S/V is the surface to volume ratio, D is the diffusion coefficient, γ the gyromagnetic ratio, G is the magnetic field gradient, and TE the echo time.

The T_2 becomes $T_{2\text{eff}}$ because the inhomogeneous B_1 and B_0 will result in an imperfect CMPG decay. A simple fitting of the $T_{2\text{eff}}$ decay data provides values that may be correlated to compressive strength development of the material [16]. This is possible since the capillary pores decrease in size as cement hydration proceeds, and the pore refinement is reflected in the relaxation times.

A Regularized Inverse Laplace Transform based on the UPEN program [17] provided the $T_{2\text{eff}}$ distributions in hydrating Portland cement mortar (Fig. 6). The shift in $T_{2\text{eff}}$ indicates a reduction of the mean pore size distribution, as expected. This permits observation of the effects of different curing regimes and mineral/chemical admixtures on the microstructure development over time. The T_2 distributions from the NMR sensor shows only one peak (Fig. 6a) which could be a result of the low signal-to-noise ratio of the data, whereas the Minispec results show two peaks with values at 1 ms and 24 ms (Fig. 6a) that correspond to the gel and capillary pores [13].

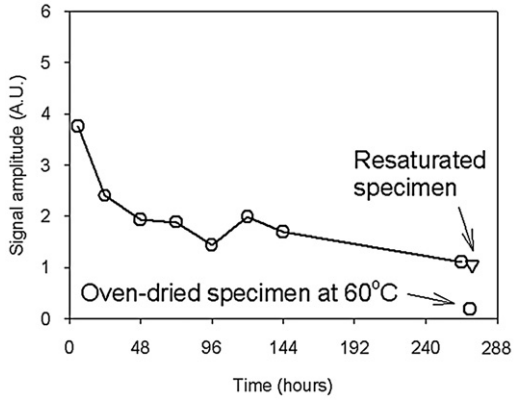

Fig. 8. Evaporable water signal loss during hydration of a sealed Portland cement mortar specimen (w/c = 0.45).

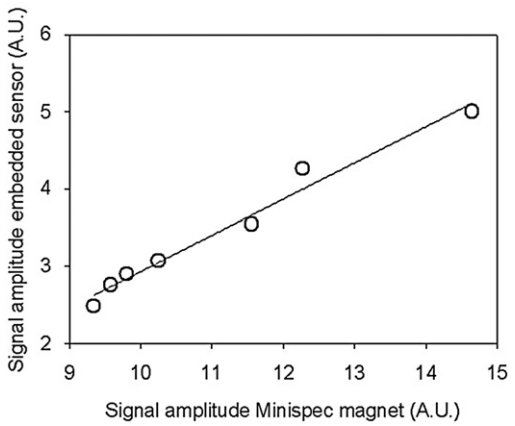

Fig. 9. Relationship between the signal detected with the embedded sensor and the signal detected in an ordinary low field magnet.

Figs. 7 and 8 show the NMR signal change caused by the loss of evaporable water during hydration of the specimens. There is a decrease in NMR signal as hydration of the cement reduces the amount of evaporable water in the sample. Oven drying the specimen to constant mass at 60 °C further reduces the amount of water. It is expected that drying at 105–110 °C would completely remove all the evaporable water. However, this range of temperature may damage the magnets. After re-saturation most of the signal is recovered.

These relative changes may be converted into absolute values (kilograms of water/cubic metres of mortar) if one knows absolute water content after placing or after a specific time by oven-drying specimens, and assuming the response of the sensor is constant over a prolonged time (e.g. months), then a simple ratio of the back

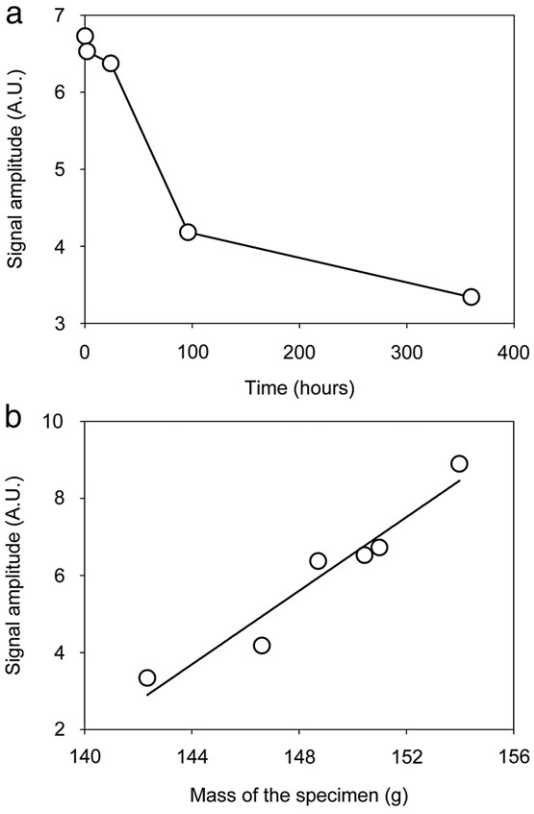

Fig. 10. a) NMR signal loss during drying of mortar w/c = 0.60 at 23 °C and 30% RH after 21 days of hydration. Because of the low water content in the sample, the number of scans was increased to 16,384 and the TR was reduced to 0.10 s>>5·T_1, with an acquisition time of 30 min; b) NMR signal vs mass of the specimen during drying.

extrapolated echoes would suffice. However, this assumption will not always be reasonable in field structures because temperature changes with season, especially in northern countries where temperature differences between seasons could be higher than 50 °C. The magnetic field of the sensors varies with these changes and it will be necessary to determine the dependence of the NMR signal on temperature of the sensors.

Fig. 9 shows a plot of the signal amplitude obtained with the miniature sensors and the signal amplitude obtained with a Bruker Minispec low field permanent magnet (0.15 T). There is a linear relationship between these values, which demonstrates the validity of the measurements made with the embedded sensor. Therefore, the signal changes detected with the miniature sensors is a measure of the evaporable water loss due to hydration of cement.

The signal loss during drying, characterized by mass loss, is shown in Fig. 10a. Fig. 10b shows the relationship between the weight of the specimen and the NMR signal detected. An improved linear relationship would be obtained with an increase in the number of scans (e.g. 30,000 with an acquisition time of 1 h) to compensate for the signal reduction caused by low water content in the specimen, or an improved sensor design.

4. Conclusions

Preliminary results of the use of miniature NMR sensors indicate the potential of these devices to monitor loss of evaporable water due to hydration/drying in cement based materials.

The NMR signal amplitude is proportional to the amount of evaporable water in fresh cement paste mixes and in hardened Portland cement mortar during drying.

The signal amplitude over time has a good linear correlation with the signal amplitude obtained in a companion sample tested in an ordinary low field magnet.

5. Future work

Future work will focus on the determination of the mechanical properties of concrete specimens to correlate with the NMR parameters measured with the embedded sensors and the evaluation of future prospects for short, medium and long term monitoring of concrete structures in situ.

Acknowledgements

BJB thanks NSERC of Canada. The UNB MRI Centre is supported by an NSERC Major Resources Support grant. P F de J Cano acknowledges the support from the Instituto Politecnico Nacional de Mexico for the sabbatical year 2007–2008, and the CONACYT from Mexico for a sabbatical scholarship.

References

[1] A.M. Neville, Properties of Concrete, Longman Group Limited, 1995.
[2] ASTM F 2170-02, Standard Test Method for Determining Relative Humidity in Concrete Floor Slabs Using In-Situ Probes, ASTM International, West Conshohocken, PA, 2002 5 pp.
[3] P. Craig, G. Donnelly, Moisture testing of concrete slabs—when 3 lbs is not 3 lbs, Concrete International 28 (2006) 23–27.
[4] ASTM F 1869-04, Standard Test Method for Measuring Moisture Vapor Emission Rate of Concrete Subfloor Using Anhydrous Calcium Chloride, ASTM International, West Conshohocken, PA, 2004 3 pp.
[5] H. Gran, E. Hansen, Effects of drying and freeze/thaw cycling probed by ^{1}H NMR, Cement and Concrete Research 27 (1997) 1319–1331.
[6] S.D. Beyea, B.J. Balcom, P.J. Prado, A.R. Cross, C.B. Kennedy, R.L. Armstrong, T.W. Bremner, relaxation time mapping of short T_2^* nuclei with single-point imaging (SPI) methods, Journal of Magnetic Resonance 135 (1998) 156–164.
[7] C. Choi, B.J. Balcom, S.D. Beyea, T.W. Bremner, P.E. Grattan-Bellew, R.L. Armstrong, Spatially resolved pore-size distribution of drying concrete with magnetic resonance imaging, Journal of Applied Physics 88 (2000) 3578–3581.
[8] S.D. Beyea, B.J. Balcom, T.W. Bremner, P.J. Prado, D.P. Green, R.L. Armstrong, P.E. Grattan-Bellew, Magnetic resonance imaging and moisture content profiles of drying concrete, Cement and Concrete Research 28 (1998) 453–463.
[9] F. de J. Cano Barrita, T.W. Bremner, B.J. Balcom, M.B. MacMillan, W.S. Langley, Moisture distribution in drying ordinary and high performance concrete cured in a simulated hot dry climate, Materials and Structures 37 (2004) 522–531.
[10] F. de J Cano Barrita, T.W. Bremner, B.J. Balcom, Effects of curing temperature on moisture distribution, drying and water absorption in compacting concrete, Magazine of Concrete Research 55 (2003) 517–524.
[11] T. Apih, A. Lahajnar, A. Sepe, R. Blinc, F. Milia, R. Cvelbar, I. Emri, B.V. Gusev, L.A. Titova, Proton spin-lattice relaxation study of the hydration of self-stressed expansive cement, Cement and Concrete Research 31 (2001) 263–269.
[12] B. Blumich, S. Anferoya, R. Pechnig, H. Pape, J. Arnold, C. Clauser, Mobile NMR for porosity analysis of drill core sections, Journal of Geophysics and Engineering 1 (2004) 177–180.
[13] J. Boguszynska, M.C.A. Brown, P.J. McDonald, J. Mitchell, M. Mulheron, J. Tritt-Goc, D.A. Verganelakis, Magnetic resonance studies of cement based materials in inhomogeneous magnetic fields, Cement and Concrete Research 35 (2005) 2033–2040.
[14] A.E. Marble, I.V. Mastikhin, B.G. Colpitts, B.J. Balcom, A constant gradient unilateral magnet for near-surface MRI profiling, Journal of Magnetic Resonance 183 (2006) 240–246.
[15] A.E. Marble, J.J. Young, I.V. Mastikhin, B.G. Colpitts, B.J. Balcom, A small, low cost embedded NMR sensor suitable for bulk measurement of porous materials, Proceedings of the Eighth International Bologna Conference on Magnetic Resonance in Porous Media, Magnetic Resonance Imaging 25 (2007) 572–573.
[16] B. Wolter, F. Kohl, N. Surkova, G. Dobmann, Practical applications of NMR in Civil Engineering, International Symposium on Non-Destructive Testing in Civil Engineering, 2003.
[17] G.C. Borgia, R.J.S. Brown, P. Fantazzini, Uniform-Penalty Inversion of Multi-exponential Decay Data, Journal of Magnetic Resonance 132 (1998) 65–77.